

# DCP-GAN: a Novel Deep Learning Network for Fingerprint Super-Resolution

Anonymous CVPR submission

Paper ID Group 4

## Abstract

001      *Fingerprint recognition is currently one of the most com-*  
002      *monly used biometric recognition technologies. At present,*  
003      *automatic fingerprint recognition systems have high accu-*  
004      *racy in identifying fingerprints with good image quality.*  
005      *However, for low-quality fingerprint images, due to the*  
006      *presence of a large amount of noise interference, it is dif-*  
007      *ficult to correctly extract features and the recognition accu-*  
008      *racy is low. Therefore, we propose a fingerprint image*  
009      *super-resolution reconstruction algorithm based on a gen-*  
010      *erative adversarial network with dense connection pyra-*  
011      *mids to address the issue of low accuracy in low-quality*  
012      *fingerprint recognition. Firstly, in order to maximize infor-*  
013      *mation sharing between convolutional layers, dense con-*  
014      *nnection blocks are added to the generator. Secondly, the*  
015      *network adds pyramid blocks containing convolutional ker-*  
016      *nels of different sizes between Dense blocks, and extracts*  
017      *features at different levels using convolutional kernels of*  
018      *different sizes. Finally, this article proposes to reconstruct*  
019      *super-resolution reconstructed images of different magnifi-*  
020      *cations based on parallel feature maps in a model. This*  
021      *multi magnification architecture can have the advantage of*  
022      *sharing underlying information during the training process.*

## 023 1. Introduction

024 Fingerprint recognition as shown in Fig.1, an impor-  
025 tant branch of biometric recognition technology for iden-  
026 tity recognition, has a long technological development  
027 history[20]. Despite the impressive results, the recogni-  
028 tion performance for low-quality fingerprint images with  
029 low resolution and noises which often have unclear ridge  
030 structures and uneven image contrast remains suboptimal.  
031 Enhancing the quality of fingerprint images is crucial for  
032 reliable identification, and a widely adopted method is  
033 through fingerprint enhancement, which removes noise and  
034 accentuates the ridge patterns. Numerous algorithms aim  
035 to improve image fidelity by reducing background noise  
036 and boosting ridge contrast, leading to enhanced recogni-  
037 tion capabilities. Although these enhancement techniques

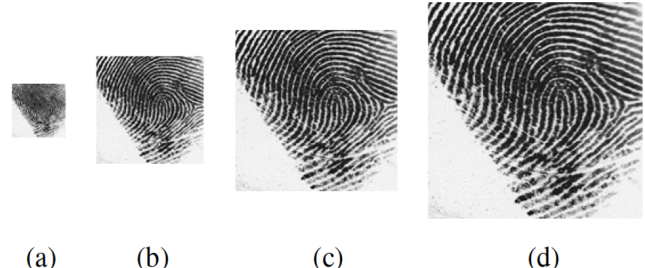


Figure 1. Fingerprint samples under different reconstruction resolutions: (a) 250 dpi, (b) 500 dpi, (c) 750 dpi, and (d) 1000 dpi.

[3, 5, 7, 18, 29] diminish noise and clarify details for more precise identification, they do not reconstruct the fine ridge details by augmenting the resolution of the image itself.

Currently, most fingerprint collection devices have a resolution of 500 dpi (Dots Per Inch). However, many low-cost or miniaturized sensors capture images at resolutions below 500 dpi. Low-resolution fingerprint images result in the loss of detailed features, thereby affecting fingerprint recognition performance[28]. Therefore, the issue of fingerprint super-resolution reconstruction[12, 24] remains a significant challenge in fingerprint processing. Additionally, when collecting infant fingerprints [1], the small area of these prints means that sensors designed for 500 dpi adult fingerprints capture images at resolutions less than 500 dpi, significantly reducing recognition performance. Using higher-resolution collection devices, on the other hand, entails higher cost implications.

Despite numerous challenges in recognizing low-quality fingerprint images, extensive research has focused on algorithms for removing background noise and enhancing fingerprint ridges to achieve better recognition performance. While fingerprint enhancement can reduce image noise and improve detail for more accurate recognition, it cannot reconstruct ridge details or recover them by increasing image resolution. Moreover, there has been limited research focused on fingerprint image super-resolution reconstruction (Super Resolution, SR) [12, 22]. Image super-resolution [15] reconstruction refers to the process of enlarging a low-

066 resolution (LR) image to a high-resolution (HR) image. It  
 067 is a crucial image processing technique in computer vi-  
 068 sion and image processing. Super-resolution reconstruction  
 069 technology has been extensively researched and applied in  
 070 computer vision tasks. The most critical issue in super-  
 071 resolution reconstruction tasks is how to reconstruct the de-  
 072 tails lost in low-resolution images.

073 The swift advancement in deep learning [31]. has led to  
 074 the emergence of various deep neural networks tailored for  
 075 image super-resolution tasks. Among these, the SRCNN  
 076 and its variant FSRCNN, were designed to perform an end-  
 077 to-end mapping from bicubic-interpolated low-resolution  
 078 images to their high-resolution counterparts. The success  
 079 of residual CNNs in this domain inspired the adoption of  
 080 the ResNet [13] architecture for image super-resolution, as  
 081 proposed in recent studies. Moreover, the field has seen in-  
 082 novations like a densely connected deep network [30] for  
 083 single-image super-resolution, capitalizing on the integra-  
 084 tion of features from various network layers to refine the  
 085 reconstruction results. Recently, the integration of genera-  
 086 tive adversarial networks (GANs) into the realm of super-  
 087 resolution has marked a significant milestone [17].

088 In the realm of computer vision, while a plethora of  
 089 methods have been developed for image super-resolution,  
 090 the specific area of fingerprint super-resolution remains un-  
 091 derexplored [1, 22, 27]. To bridge this gap, this study intro-  
 092 duces an innovative approach, the Dense Connected Pyra-  
 093 mid Generative Adversarial Network (DCP-GAN), tailored  
 094 for enhancing the resolution of fingerprint images across  
 095 multiple scales. This approach leverages the strides made  
 096 in deep learning for image super-resolution.

097 The methodology encompasses two distinct stages: of-  
 098 fline training and online testing. The offline training phase  
 099 begins with the collection of a substantial dataset of high-  
 100 resolution fingerprint images (1000 dpi), which form the  
 101 foundation for generating lower resolution counterparts  
 102 through a downsampling process. Following this, the DCP-  
 103 GAN is meticulously designed. It features a sophisticated  
 104 generator network with dense connected pyramidal archi-  
 105 tecture, focused on the intricate task of image reconstruc-  
 106 tion. Complementing this is a feature-consistent discrimi-  
 107 nator, fine-tuned to enhance the model’s accuracy. The net-  
 108 work undergoes rigorous super-resolution training utilizing  
 109 paired datasets, honing its ability to discern and enhance hi-  
 110 erarchical features in the transformation from low to high-  
 111 resolution fingerprints. During the online testing phase, this  
 112 meticulously trained super-resolution network is deployed  
 113 to generate fingerprints of significantly enhanced resolu-  
 114 tion. The primary contributions of this paper are summa-  
 115 rized as follows.

- 116 • We present a novel fingerprint image super-resolution  
 117 framework based on a Generative Adversarial Network  
 118 (GAN) structure. This framework is adept at learning and

119 combining features across different levels, resulting in  
 120 a highly effective high-resolution fingerprint reconstruc-  
 121 tion.

- 122 • We introduce a dense connected pyramid generative ad-  
 123 versarial network specifically designed for the reconstruc-  
 124 tion of high-resolution fingerprint images. This deep net-  
 125 work comprises a dense connected pyramid generator for  
 126 image reconstruction and a feature-consistent discrimi-  
 127 nator. This marks the first application of GAN’s deep  
 128 network architecture in the realm of fingerprint super-  
 129 resolution.
- 130 • Our approach achieves state-of-the-art results in both vi-  
 131 sual inspection and fingerprint recognition performance.  
 132 This success is evident not only in adult FVC finger-  
 133 print databases but also in challenging child fingerprint  
 134 databases. The performance improvements escalate with  
 135 larger upscaling factors, making this the first work to  
 136 demonstrate that image super-resolution can effectively  
 137 enhance the recognition of challenging child fingerprints.

138 The rest structure of the paper is as follows: Section 2  
 139 describes the relevance work. Section 3 provides a detailed  
 140 description of the proposed fingerprint super-resolution al-  
 141 gorithm. Section 4 discusses our experimental setup and  
 142 the results obtained. Finally, in Section 5, we conclude the  
 143 paper with a summary of our findings and contributions.

## 2. Related Work

### 2.1. Low-quality fingerprint images processing

144 Before the rapid development of machine learning, finger-  
 145 print image enhancement typically utilized Gabor filtering  
 146 algorithms[14]. Given that fingerprint images have dis-  
 147 tinct frequencies and orientations in their ridge and val-  
 148 ley patterns, Gabor filters[14], known for their selectivity  
 149 in frequency and orientation, were extensively researched  
 150 for optimization in fingerprint enhancement. Feng *et al.*  
 151 [11]proposed a method based on Gabor filtering to estimate  
 152 the local ridge orientations in enhanced fingerprint images.  
 153 Additionally, Chikkerur *et al.*[6] introduced a technique for  
 154 fingerprint enhancement using two-dimensional Short Time  
 155 Fourier Transform (STFT) analysis in the frequency do-  
 156 main. This method involves using STFT to estimate the  
 157 probability of ridge directions and frequencies, ultimately  
 158 enhancing the fingerprint based on these orientations, fre-  
 159 quencies, and angles.

160 Beyond these, enhancement methods based on the To-  
 161 tal Variation (TV) [32, 33] image model were also com-  
 162 monly used for fingerprint images. These methods decom-  
 163 pose low-quality fingerprint images into texture and cartoon  
 164 components. Building on this, a model based on Adap-  
 165 tive Directional Total-Variation (ADTV) was proposed [33].  
 166 This model enhances low-quality fingerprint images by in-  
 167 tegrating scale and directional features to eliminate struc-

tured noise. As machine learning technology continued to evolve, Dictionary Learning was first applied in studies related to the enhancement of low-quality fingerprint images. Cao *et al.* [4] developed a dictionary learning-based method to estimate the orientation and frequency fields of low-quality fingerprint images for enhancement. Moreover, Liu *et al.* [19] proposed a method using sparse representation of multi-scale image blocks for the segmentation and enhancement of low-quality fingerprint images. In this method, Gabor elementary functions were used to build a dictionary, and a sparse representation method based on multi-scale image blocks was iteratively applied to reconstruct fingerprint images.

## 2.2. Super-resolution reconstruction of deep convolutional neural networks

Although research on super-resolution reconstruction[31] of fingerprint images is scarce, a vast array of super-resolution reconstruction methods based on deep convolutional neural networks (CNNs) has been proposed in the field of computer vision. A critical aspect of this study is to explore how these novel super-resolution deep CNNs can be applied to the super-resolution reconstruction of fingerprint images. A deep CNN named SRCNN (Super-Resolution Convolutional Neural Network) [9] was the first to apply deep learning methods to image super-resolution tasks. This algorithm initially enlarges low-resolution images using bicubic interpolation and then employs three convolutional layers for feature extraction and representation, non-linear mapping, and reconstruction. In 2016, an improved version of SRCNN, known as FSRCNN (Fast Super-Resolution Convolutional Neural Network)[10], was proposed. This model inputs low-resolution images directly into the neural network and uses deconvolution operations to upscale the image, directly outputting high-resolution images. Shi *et al.*[25] proposed an enhanced structure, ESRPCN (Efficient Sub-Pixel Convolutional Network), which replaces deconvolution layers with a sub-pixel convolution layer, rearranging feature maps to increase image resolution.

Kim *et al.*[13] introduced the ResNet structure into super-resolution reconstruction networks, proposing VDSR (Very Deep Super-Resolution)[15]. Building on this, Tong *et al.*[30], drawing inspiration from the DenseNet structure, proposed SRDenseNet, which deepens the network layers and tested three scales of SRDenseNet structures. Lai *et al.*[16] addressed the issues faced by single magnification super-resolution networks at high magnifications (such as 8x) and proposed LapSRN (Laplacian Pyramid Super-Resolution Network). Addressing the problem of high-frequency detail loss in super-resolution reconstruction tasks, Ledig *et al.*[17] introduced SRGAN (Super-Resolution Generative Adversarial Network), which uses

content loss functions and adversarial loss functions to enhance the visual effect of super-resolution reconstruction images. This comprehensive exploration of deep learning-based super-resolution techniques opens up new possibilities for enhancing the resolution of fingerprint images, a crucial aspect of biometric security and identification.

## 3. Methodology

### 3.1. Overview of the Proposed Algorithm

In this research, we focus on the deep learning-driven transformation of low-resolution (LR) to high-resolution (HR) fingerprint images using the Densely Connected Pyramid Generative Adversarial Network (DCP-GAN). Our approach is encapsulated in a comprehensive framework, illustrated in Fig.2, which outlines the process encompassing both offline training and online testing stages. Initially, in the offline training, we curate paired datasets of LR and HR fingerprint images. Subsequently, in the online testing phase, the network utilizes the learned mapping to process LR inputs and generate super-resolved HR fingerprint images. The ultimate goal of DCP-GAN is to master the intricacies of fingerprint details, enhancing the image quality for improved identification accuracy.

### 3.2. The Densely Connected Pyramid Generative Adversarial Networks (DCP-GAN)

In this study, we introduce a novel approach for fingerprint image enhancement using a Densely Connected Pyramid Generative Adversarial Network (DCP-GAN). This network employs a multi-level feature-extracting generator for image super-resolution and a discriminator that discerns the authenticity of the generated images. The adversarial process continues until a Nash equilibrium is reached, allowing the generator to create highly realistic high-resolution fingerprints. The detailed structures of both the generator and the discriminator will be discussed in subsequent sections, with their architectures depicted in Fig.3.

#### 3.2.1 Densely Connected Pyramid Generator

Super-resolution networks differ from U-net structures in image segmentation, as they directly apply convolutions at high resolutions rather than using encoder-decoder architectures. Initially, these networks employed bicubic interpolation for upscaling, followed by convolution for reconstruction, leading to higher computational and memory demands due to the high-dimensional operations involved. To minimize high computational and memory costs, the network inputs low-resolution images and employs a deep convolutional network to learn and extract features, followed by an upsampling layer at the end for high-resolution reconstruction, forming the generator. The generator's architecture is

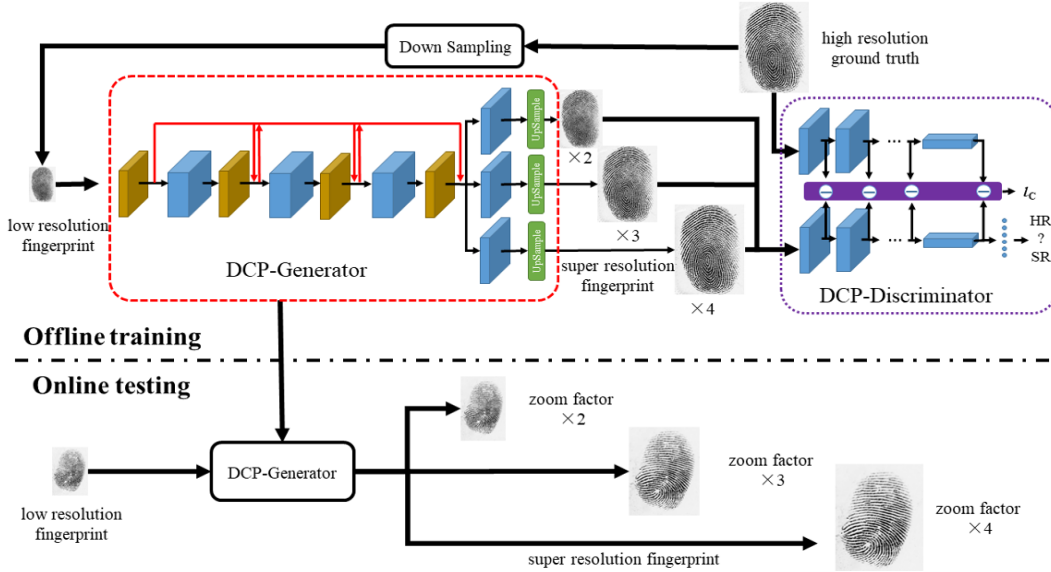


Figure 2. The whole framework of our proposed method for enhancing fingerprint images from low to high resolution using DCP-GAN.

showcased in Fig.3(a).

**Dense Blocks for Enhanced Information Sharing:** The generator incorporates Dense Blocks to maximize inter-layer information sharing, contrasting with ResNet's direct feature map summation. Short paths are established between each layer and every other layer in DenseNet, enhancing robust information and mitigating the vanishing-gradient problem. The introduced Dense Blocks concatenate feature maps from preceding layers, each containing 6 convolutional layers with a  $1\times 1$  bottleNeck layer,  $3\times 3$  convolution layer, and batch normalization, activated by LeakyReLU. Skip connections between these blocks facilitate feature fusion across levels.

**Pyramid Blocks for Multi-Scale Feature Capturing:** DCP-GAN introduces Pyramid Blocks, and each Pyramid Block employs four kernel sizes ( $3\times 3$ ,  $5\times 5$ ,  $7\times 7$ ,  $9\times 9$ ) in parallel to integrate image details across various scales. Additionally, akin to DenseNet, we also employ a Dense block to densely connect the outputs between two pyramid blocks, which effectively harnesses information from various network layers, facilitating the construction of a densely connected pyramid generator. Subsequently, the concatenated feature maps from all pyramid blocks serve as input for the subsequent upsampling and reconstruction blocks.

**Efficient Multi-Scale Upsampling:** The model features a multi-scale architecture for different magnification levels, sharing foundational information during training. The upsampling layer uses sub-pixel convolution (PixelShuffle Layer) with a stride of  $r$  which denotes the upscaling zoom factor, more efficient than deconvolution, for rearranging the feature maps of size  $W \times H \times (C \times r^2)$  to a

high-resolution image of  $Wr \times Hr \times C$ . The DCP-GAN's three output layers set the scaling factor  $r$  to 2, 3, and 4 for 2x, 3x, and 4x magnification, respectively. For instance, a  $128\times 128$  input is upscaled to outputs of  $256\times 256$ ,  $384\times 384$ , and  $512\times 512$ .

### 3.2.2 Discriminator Network

In the DCP-GAN framework, the discriminator plays a crucial role, tasked with distinguishing between authentic high-resolution fingerprint images and super-resolution reconstructed images produced by the generator. Given the generator's capability to create super-resolution images at three different magnification levels, three distinct discriminators are designed, each tailored to a specific resolution. As illustrated in Fig.3(b), each discriminator is equipped with eight convolutional modules. These modules are a concatenation of a convolutional layer, batch normalization, LeakyReLU activation, and a maxpooling layer. The convolutional layers across all modules feature a kernel size of  $3 \times 3$  and a stride of  $1 \times 1$ . Except for the first maxpooling layer, all others are sized at  $2 \times 2$ . For discriminators targeting magnification levels of 2x, 3x, and 4x, the first maxpooling layers are sized at  $2 \times 2$ ,  $3 \times 3$ , and  $4 \times 4$ , respectively. Following the convolutional layers, the network integrates a fully connected layer and a Sigmoid activation layer to output the classification result. An input of an authentic high-resolution image results in an output of 1, whereas a super-resolution reconstructed image yields an output of 0. Beyond the final output layer, this study also extracts intermediate feature layers, enhancing the discriminator's ability

301  
302  
303  
304  
305

306  
307  
308  
309  
310  
311  
312  
313  
314  
315  
316  
317  
318  
319  
320  
321  
322  
323  
324  
325  
326  
327  
328  
329

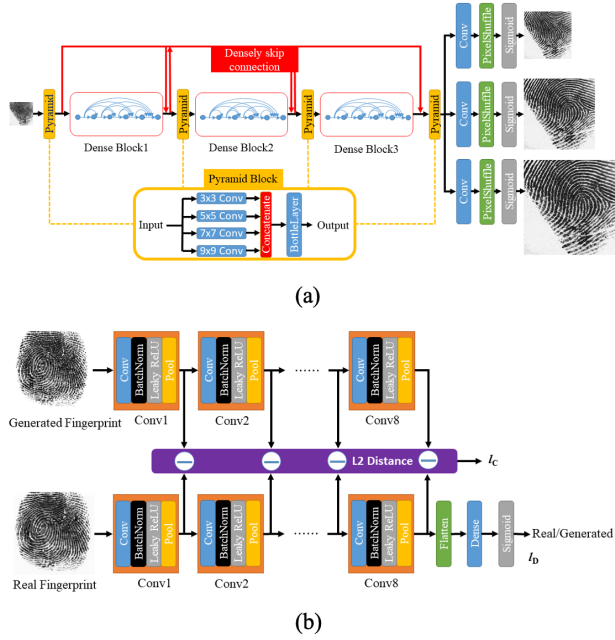


Figure 3. Two main components of the DCP-GAN architecture for fingerprint image super-resolution: (a) the densely connected pyramid generator, which is responsible for image reconstruction, and (b) the feature consistent discriminator, which evaluates the authenticity of the generated images.

330 to identify fingerprint features.

### 3.3. Loss Function

332 In order to quantitatively assess the effectiveness of the  
 333 generated images and the performance of the network, the  
 334 DCP-GAN model incorporates the Mean Squared Error  
 335 (MSE) and the Structural Similarity Index (SSIM) as part  
 336 of its loss function. The MSE measures the pixel-level dif-  
 337 ferences between the super-resolution image and the original  
 338 high-resolution image. Conversely, SSIM evaluates the  
 339 structural similarity between the two images. The loss func-  
 340 tion of the discriminator in the DCP-GAN model for a sin-  
 341 gle image is shown as follows:

$$342 \quad \mathcal{L}_G = MSE(S, H) + \lambda_1 \frac{1}{N} \sum_{p=1}^N SSIM(S_p, H_p) \quad (1)$$

343 where  $S$  and  $H$  are the super-resolution and ground truth  
 344 high-resolution fingerprint images,  $S_p$  and  $H_p$  are the local  
 345 neighborhoods of pixel  $p$  in the generated and ground truth  
 346 images;  $N$  denotes the total number of pixels in the finger-  
 347 print image, and  $\lambda_1$  is a parameter used to adjust the weights  
 348 of the Mean Squared Error (MSE) and the Structural Simi-  
 349 larity Index (SSIM).

In addition to the adversarial loss, the DCP-GAN model utilizes a feature consistency loss, referenced in [23], to ensure that the super-resolution reconstructed images maintain consistency with the real high-resolution fingerprint images in terms of the hierarchical feature maps generated by the discriminator. The feature consistency loss is defined as:

$$350 \quad \mathcal{L}_C = \sum_{s=1}^M ||F_s(S)) - F_s(H)|| \quad (2)$$

351 where  $M$  is the number of feature vectors, and  $F_s$  repre-  
 352 sent the image feature vector generated by the discrimi-  
 353 nator. The objective during the training of the generator is  
 354 to minimize the distance between the feature vectors of the  
 355 generated images and those of the authentic high-resolu-  
 356 tion images. Conversely, the training objective for the discrimi-  
 357 nator is the opposite.

358 The adversarial loss is used to improve the ability of  
 359 the discriminator to differentiate between authentic high-  
 360 resolution fingerprint images and the super-resolution recon-  
 361 structed images produced by the generator. The adver-  
 362 sarial loss is formally defined as:

$$363 \quad \mathcal{L}_D = E_{H \sim p_H} [\log(D(H))] + E_{L \sim p_L} [1 - \log(D(G(L)))] \quad (3)$$

364 where  $H$  is the high-resolution fingerprint as input of the  
 365 discriminator and  $L$  is the low-resolution fingerprint as input  
 366 of the generator;  $G(\cdot)$  is the output of the generator and  
 367  $D(\cdot)$  is the output of the discriminator;  $E(\cdot)$  denotes the  
 368 expectation operator. The discriminator is tasked with classi-  
 369 fying whether the input image is generated or a real high-  
 370 resolution fingerprint and thus its output is a binary value.

371 Finally, the content loss, feature consistency loss, and ad-  
 372 versarial loss are integrated to formulate the complete loss  
 373 function for the DCP-GAN model. The combined loss func-  
 374 tion is defined as:

$$375 \quad \mathcal{L}_{DCP-GAN} = \mathcal{L}_G + \lambda_2 (\mathcal{L}_C + \mathcal{L}_D) \quad (4)$$

376 where  $\lambda_2$  is a parameter that balances the content loss and  
 377 the adversarial loss. The final aim is to train the network to  
 378 generate super-resolution images that are structurally and  
 379 feature-wise similar to the original high-resolution images.

## 380 4. Experiments

### 381 4.1. Datasets

382 This chapter mainly uses the FVC database, fingerprint  
 383 database of young children, and adult high-resolution fin-  
 384 gerprint database for related algorithm research. The adult  
 385 high-resolution fingerprint database is mainly used for deep  
 386 neural network training data, while the FVC database and

394 fingerprint database of young children are mainly used for  
 395 algorithm performance verification.

396 **FVC Database:** FVC databases are generally high-  
 397 quality, and the official fingerprint matching standards are  
 398 provided, making it a popular database for fingerprint  
 399 matching algorithm research. The number of images in each  
 400 database is 100 fingers in database A, 10 fingers in database  
 401 B, and 8 images of each finger, collected by different sensors,  
 402 with a resolution of about 500 dpi. To better compare  
 403 with other methods, we choose FVC2000DB3\_B and  
 404 FVC2004DB3\_B in our experiments.

405 **Fingerprint Database of Young Children:** Due to the  
 406 smaller size and edge structure of young children's finger-  
 407 prints compared to adults, if existing methods are directly  
 408 used, the accuracy of young children's fingerprint recogni-  
 409 tion is lower than that of adults. Therefore, we established a  
 410 fingerprint database collected from 200 fingers of 2-5 year  
 411 old children to test the proposed algorithm. Figure 5 shows  
 412 some examples of fingerprint images from the fingerprint  
 413 database. The size of each fingerprint image is  $600 \times 800$ ,  
 414 with a resolution of 1000 dpi. This fingerprint database  
 415 contains 2000 1000dpi fingerprint images from 200 fingers,  
 416 with 10 images per finger.

417 **High Resolution Fingerprint Database:** To train the  
 418 proposed deep networks, a large number of training data is  
 419 required including the paired low and high resolution finger-  
 420 print images, so we additionally collected and established a  
 421 high-resolution fingerprint database. This database uses an  
 422 optical single finger fingerprint capture device to capture  
 423 single finger fingerprint images of volunteers, with an im-  
 424 age size of 600x800 pixels, with a resolution of 1000dpi.

## 425 4.2. Experimental protocol

426 The DCP-GAN model proposed in this algorithm is built  
 427 using Python programming language and PyTorch deep  
 428 learning framework. Hardware environment usage Intel  
 429 Xeon E5-2620v4@2.1GHz CPU And use NVIDIA  
 430 GeForce RTX2080Ti GPU for acceleration operations. The  
 431 model is trained using an Adam optimizer with an initial  
 432 learning rate set to 0.001.

433 This chapter first conducts network structure ablation ex-  
 434 periments on deep convolutional neural networks, mainly to  
 435 verify the effectiveness of the proposed DCP-GAN partial  
 436 structure in this chapter. The validation structures mainly  
 437 include DenseBlock, PyramidBlock, and generative adver-  
 438 sarial structures. Firstly, the generative adversarial part of  
 439 DCP-GAN is removed, and only the content loss function  
 440 used by the generator is retained. This structure is called  
 441 DCP-Net; Next, remove PyramidBlock from the network  
 442 structure, which is called DC Net. Finally, remove the  
 443 DenseBlock from the network, and the network structure  
 444 is called SR Net. Train SRNet, DC Net, DCP Net, and  
 445 DCP GAN using the same training data to compare the per-

Network	PSNR			SSIM		
	500dpi	750dpi	1000dpi	500dpi	750dpi	1000dpi
SRNet	24.62	24.50	24.48	0.9012	0.8941	0.8853
DC-Net	27.13	26.93	26.85	0.9040	0.8999	0.8939
DCP-Net	27.52	27.32	27.24	0.9088	0.9035	0.8973
DCP-GAN	27.76	27.54	27.44	0.9111	0.9037	0.8977

Table 1. Psnr and ssim of different network structures on finger-  
 print database of young children.

446 formance differences of different network structures. The  
 447 network structure ablation experiment mainly compares the  
 448 peak signal-to-noise ratio (PSNR) and structural similarity  
 449 (SSIM) of the image.

450 This experiment uses the FVC database and finger-  
 451 print database of young children to verify the effectiveness of  
 452 different super-resolution reconstruction methods on finger-  
 453 print matching. To facilitate comparison with other literature,  
 454 this article uses the open-source C# finger-  
 455 print matching algorithm architecture. The matching algorithm uses  
 456 M3gl[21] and adopts the same matching scheme: pairwise  
 457 matching of the same finger, matching of different fingers  
 458 using the same number, all images are downsampled to  
 459 low resolution by magnification, and then reconstructed to  
 460 500dpi by super-resolution for matching. The accuracy in-  
 461 dex of matching is mainly obtained through the Detection  
 462 Error Trade off (DET) curve. The main indicator of the  
 463 curve is Equal Error Rate (EER). This experiment evaluates  
 464 the super-resolution reconstruction effect through the above  
 465 matching indicators, and the error rate parameters are as low  
 466 as possible.

## 467 4.3. Ablation Study on Network Architecture

468 This section uses a high-resolution fingerprint database of  
 469 1000dpi for ablation experiments to verify the effectiveness  
 470 of different network structures. Table1 shows the PSNR and  
 471 SSIM indicators of high-resolution fingerprint databases  
 472 with different network structures. It can be seen that as the  
 473 network structure becomes more complex, the PSNR and  
 474 SSIM gradually improve.

475 Fig.4 shows an example image of super-resolution re-  
 476 construction of fingerprint images with different network  
 477 structures. From the figure, it can be seen that the images  
 478 generated by SRNet have significant texture direction er-  
 479 rors. The overall ridge direction field of the image generated  
 480 by DC Net is basically accurate, but the adhesion of adja-  
 481 cent ridges leads to the appearance of incorrect ridges. The  
 482 image lines generated by DCP Net are basically correct, but  
 483 there are still errors in the detailed features. The image lines  
 484 generated by DCP-GAN have accurate orientation, better  
 485 restoring detailed features, and are closer to the target im-  
 486 age. Through the above experiments, it has been proven that  
 487 the addition of Dense Block, Pyramid Block, and Genera-

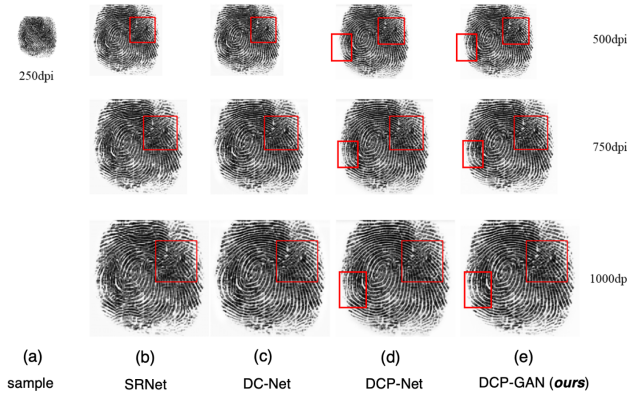


Figure 4. A sample of a 250 dpi low-resolution fingerprint and corresponding 500, 750, and 1000 dpi high-resolution images enhanced by different networks on FVC2000 DB3\_B 101\_1.

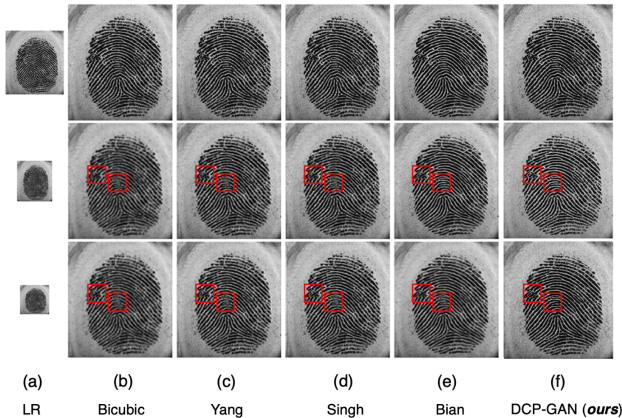


Figure 5. The low-resolution fingerprints of FVC2000DB3\_B 101\_1 downsampled by scale factors of 2, 3 and 4 from row 1 to 3 and the corresponding super-resolution results of 500 dpi generated by using different methods.

488      effective Adversarial Structure can effectively improve the effectiveness of fingerprint super-resolution reconstruction.  
489

#### 4.4. Comparison with other methods

491      In this experiment, we compare the proposed deep learning  
492      based method with other methods including the Bicubic inter-  
493      polation method and the Yang's method for fingerprint  
494      image super resolution on both the fingerprint database of  
495      young children and FVC database.

##### 4.4.1 FVC database

497      Fig.5 shows the comparison of FVC2000DB3\_B super-  
498      resolution reconstructed images generated by different  
499      methods. From the figure, it can be seen that the image  
500      generated by Bicubic is blurred. The images generated by  
501      Yang[8], Singh[26], and Bian[2] have higher sharpness, but

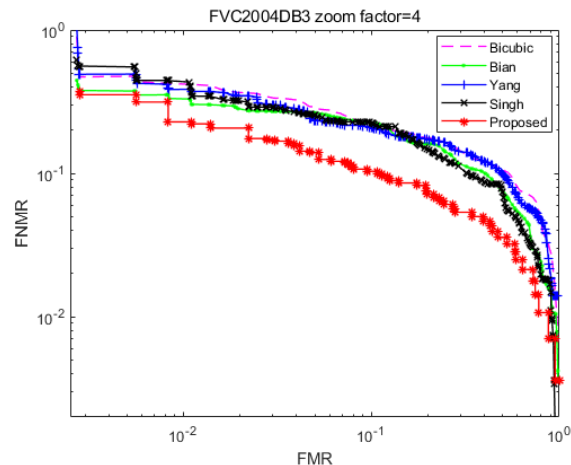


Figure 6. Comparison of the DET curves by different super-resolution methods with zoom factor 4 on FVC2000DB3\_B.

Metrics	zoom factor	Method				
		Bicubic	Bian	Yang	Singh	Proposed
EER	×2	8.31	5.46	8.31	6.17	<b>4.52</b>
(%)	×3	9.98	8.73	9.09	10.81	<b>7.04</b>
	×4	17.22	16.09	17.18	17.04	<b>9.76</b>

Table 2. Comparison of EER of different zoom factors with different super resolution methods on FVC2000DB3\_B.

they all have the problem of losing details, and Bian's results have more loss of grayscale information. The DCP-GAN image proposed in this article is clearer and can better preserve detailed information.

In terms of fingerprint matching, this article conducted matching tests using the FVC2004DB3B database, and the matching DET curve is shown in Fig.6. The EER performance indicators are shown in Table 2. Due to the experimental approach of downsampling by magnification and reconstructing the super-resolution to 500dpi, the higher the magnification, the smaller the input image size and the greater the difficulty. Therefore, the higher the magnification, the higher the error rate of the experimental results. From Fig.6, it can be seen that the image DET curve generated by DCP-GAN is lower than that of the bicubic interpolation. From Table 2, it can be seen that compared to the bicubic interpolation, the EER of DCP-GAN at 2, 3, and 4 times magnification decreased from 5.46%, 8.73%, and 16.09% to 4.39%, 7.04%, and 9.76%, respectively. The larger the magnification, the more obvious the advantage.

##### 4.4.2 Fingerprint Database of Young Children

This section evaluates various super-resolution algorithms using fingerprint database of young children. Fig.7 displays

502  
503  
504  
505  
506  
507  
508  
509  
510  
511  
512  
513  
514  
515  
516  
517  
518  
519  
520  
521

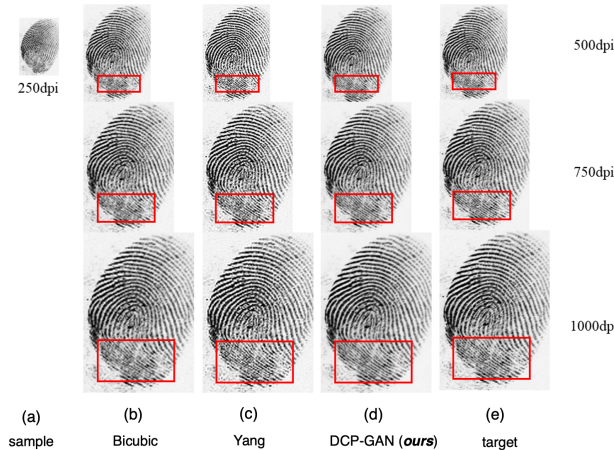


Figure 7. A sample of low-resolution fingerprint of 250 dpi and the super resolution results of 500, 750 and 1000 dpi from the first to the third row by using different methods on fingerprint database of young children.

Metrics	dpi	Method			
		Bicubic	Yang	Original	<b>Proposed</b>
EER (%)	500	9.45	8.12	7.42	<b>7.87</b>
	750	7.00	6.24	4.96	<b>5.77</b>
	1000	6.26	5.61	4.15	<b>4.95</b>

Table 3. Comparison of EER on the young children fingerprint images of different resolutions by different super resolution methods.

high-resolution young children fingerprint images produced by different methods. Notably, the Bicubic enlargement appears blurry, especially in densely textured areas (red box), hindering detailed feature distinction. Yang[8]’s enlargement exhibits improved sharpness but introduces severe noise, leading to unclear texture in the red box due to line accumulation. Contrastingly, DCP-GAN produces significantly clearer images, demonstrating high sharpness and smooth edges in sparse textures and effectively distinguishing ridges even in densely textured areas.

Subsequently, fingerprint matching is conducted on the infant database, resulting in DET curves (Fig.8) illustrating DCP-GAN’s superiority over Bicubic and Yang, aligning closely with the target high-resolution curve. Tables 3 present EER performance indicators, showing DCP-GAN outperforming other methods. For infants aged 0-2, DCP-GAN achieves EERs of 29.79%, 26.69%, and 26.19%, surpassing Yang’s 31.78%, 29.27%, and 29.29%. Similarly, for 2-5-year-olds, DCP-GAN achieves EERs of 7.87%, 5.77%, and 4.95%, outperforming Yang’s 8.12%, 6.24%, and 5.61%. Notably, DCP-GAN’s advantage becomes more pronounced with higher magnification and demonstrates lower matching error rates, emphasizing the efficacy of high

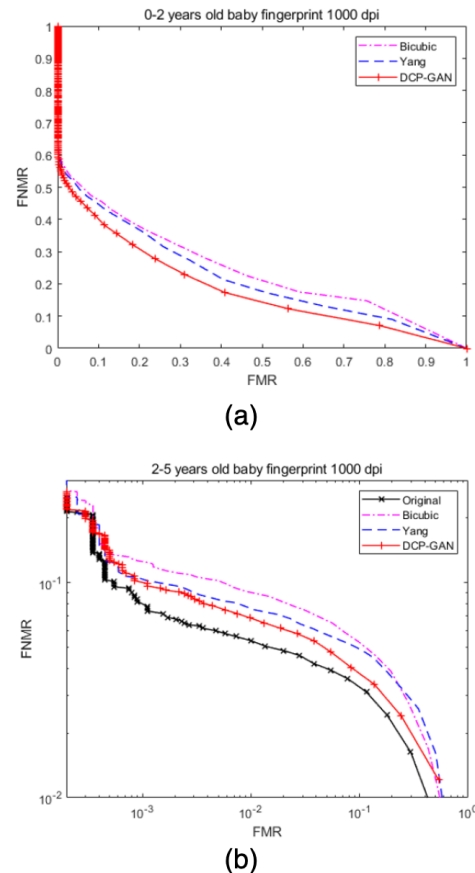


Figure 8. Comparison of the DET curves by different super-resolution methods with zoom factor 4 on young children fingerprint images.

dpi in reducing errors.

## 5. Conclusion

This paper has presented a densely connected pyramid generative adversarial network (DCP-GAN) for finger print super-resolution. The deep network of DCP-GAN consists of a densely connected pyramid generator for image reconstruction and a feature consistent discriminator for distinguish the input image as generated or real. The densely skip connections and pyramid convolution block are added to make the full use of multi-level features for reconstruction of high resolution fingerprints. In discriminator, a feature consistent component is added to enforce the feature consistency between the generated and real fingerprints. The proposed method is tested on the fingerprint database of young children and FVC database. The experiment results show that the proposed method achieved better performance than other methods. The super resolution method can provide an effective way to enhance the fingerprint recognition of young children.

567

## References

568

569

570

571

572

573

574

575

576

577

578

579

580

581

582

583

584

585

586

587

588

589

590

591

592

593

594

595

596

597

598

599

600

601

602

603

604

605

606

607

608

609

610

611

612

613

614

615

616

617

618

619

620

621

622

623

- [1] Weixin Bian, Shifei Ding, and Yu Xue. Fingerprint image super resolution using sparse representation with ridge pattern prior by classification coupled dictionaries. *IET Biometrics*, 6(5):342–350, 2016. [1](#) [2](#)
- [2] Weixin Bian, Shifei Ding, and Yu Xue. Fingerprint image super resolution using sparse representation with ridge pattern prior by classification coupled dictionaries. *Iet Biometrics*, 6 (5):342–350, 2017. [7](#)
- [3] Kai Cao and Anil K Jain. Automated latent fingerprint recognition. *IEEE transactions on pattern analysis and machine intelligence*, 41(4):788–800, 2018. [1](#)
- [4] K Cao, E Liu, and A K Jain. Segmentation and enhancement of latent fingerprints: A coarse to fine ridgestructure dictionary. *IEEE Transactions on Pattern Analysis and Machine Intelligence*, 36(9):1847–1859, 2014. [3](#)
- [5] Kai Cao, Dinh-Luan Nguyen, Cori Tymoszek, and Anil K Jain. End-to-end latent fingerprint search. *IEEE Transactions on Information Forensics and Security*, 15:880–894, 2019. [1](#)
- [6] S Chikkerur, V Govindaraju, and A N Cartwright. Fingerprint image enhancement using stft analysis. In *International Conference on Pattern Recognition and Image Analysis*, pages 20–29, 2005. [2](#)
- [7] Tarang Chugh, Kai Cao, Jiayu Zhou, Elham Tabassi, and Anil K Jain. Latent fingerprint value prediction: Crowd-based learning. *IEEE Transactions on Information Forensics and Security*, 13(1):20–34, 2017. [1](#)
- [8] Bhabesh Deka, Helal Mullah, and Avv Prasad. Fast multispectral image super-resolution via sparse representation. In *2019 2nd International Conference on Innovations in Electronics, Signal Processing and Communication (IESC)*, 2019. [7](#) [8](#)
- [9] Chao Dong, Chen Change Loy, Kaiming He, and Xiaou Tang. Learning a deep convolutional network for image super-resolution. In *European conference on computer vision*, pages 184–199. Springer, 2014. [3](#)
- [10] Chao Dong, Chen Change Loy, and Xiaou Tang. Accelerating the super-resolution convolutional neural network. In *European conference on computer vision*, pages 391–407. Springer, 2016. [3](#)
- [11] J Feng, J Zhou, and A K Jain. Orientation field estimation for latent fingerprint enhancement. *IEEE Transactions on Pattern Analysis and Machine Intelligence*, 35(4):925–940, 2012. [2](#)
- [12] Muhammad Haris, Greg Shakhnarovich, and Norimichi Ukita. Task-driven super resolution: Object detection in low-resolution images. *arXiv preprint arXiv:1803.11316*, 2018. [1](#)
- [13] Kaiming He, Xiangyu Zhang, Shaoqing Ren, and Jian Sun. Deep residual learning for image recognition. In *Proceedings of the IEEE conference on computer vision and pattern recognition*, pages 770–778, 2016. [2](#) [3](#)
- [14] L Hong, Y Wan, and A Jain. Fingerprint image enhancement: algorithm and performance evaluation. *IEEE Transactions on Pattern Analysis and Machine Intelligence*, 20(8):777–789, 1998. [2](#)

- [15] Jiwon Kim, Jung Kwon Lee, and Kyoung Mu Lee. Accurate image super-resolution using very deep convolutional networks. In *Proceedings of the IEEE conference on computer vision and pattern recognition*, pages 1646–1654, 2016. [1](#) [3](#)
- [16] W S Lai, J B Huang, N Ahuja, et al. Deep laplacian pyramid networks for fast and accurate super-resolution. In *Proceedings of the IEEE conference on computer vision and pattern recognition*, pages 624–632, 2017. [3](#)
- [17] Christian Ledig, Lucas Theis, Ferenc Huszár, Jose Caballero, Andrew Cunningham, Alejandro Acosta, Andrew Aitken, Alykhan Tejani, Johannes Totz, Zehan Wang, et al. Photo-realistic single image super-resolution using a generative adversarial network. In *Proceedings of the IEEE conference on computer vision and pattern recognition*, pages 4681–4690, 2017. [2](#) [3](#)
- [18] Jian Li, Jianjiang Feng, and C-C Jay Kuo. Deep convolutional neural network for latent fingerprint enhancement. *Signal Processing: Image Communication*, 60:52–63, 2018. [1](#)
- [19] M Liu, X Chen, and X Wang. Latent fingerprint enhancement via multi-scale patch-based sparse representation. *IEEE Transactions on Information Forensics and Security*, 10(1):6–15, 2014. [3](#)
- [20] Davide Maltoni, Dario Maio, Anil K Jain, and Salil Prabhakar. *Handbook of fingerprint recognition*. Springer Science & Business Media, 2009. [1](#)
- [21] Miguel Angel Medina-Pérez, Milton García-Borrotto, Andres Eduardo Gutierrez-Rodríguez, and Leopoldo Altamirano-Robles. Improving fingerprint verification using minutiae triplets. *Sensors*, 12(3):3418–3437, 2012. [6](#)
- [22] Ajnas Muhammed and Alwyn Roshan Pais. A novel fingerprint image enhancement based on super resolution. In *2020 6th International Conference on Advanced Computing and Communication Systems (ICACCS)*, pages 165–170. IEEE, 2020. [1](#) [2](#)
- [23] Y Pan, M Liu, C Lian, et al. Disease-image specific generative adversarial network for brain disease diagnosis with incomplete multi-modal neuroimages. In *International Conference on Medical Image Computing and Computer-Assisted Intervention*, pages 137–145, 2019. [5](#)
- [24] Mehdi SM Sajjadi, Bernhard Scholkopf, and Michael Hirsch. Enhancenet: Single image super-resolution through automated texture synthesis. In *Proceedings of the IEEE International Conference on Computer Vision*, pages 4491–4500, 2017. [1](#)
- [25] W Shi, J Caballero, F Huszár, et al. Real-time single image and video super-resolution using an efficient sub-pixel convolutional neural network. In *Proceedings of the IEEE conference on computer vision and pattern recognition*, pages 1874–1883, 2016. [3](#)
- [26] Kuldeep Singh, Anubhav Gupta, and Rajiv Kapoor. Fingerprint image super-resolution via ridge orientation-based clustered coupled sparse dictionaries. *Journal of Electronic Imaging*, 24(4):043015, 2015. [7](#)
- [27] Kuldeep Singh, Anubhav Gupta, and Rajiv Kapoor. Fingerprint image super-resolution via ridge orientation-based clustered coupled sparse dictionaries. *Journal of Electronic Imaging*, 24(4):043015, 2015. [2](#)

- 682 [28] Hong-Ren Su, Kuang-Yu Chen, Wei Jing Wong, and Shang-  
683 Hong Lai. A deep learning approach towards pore extraction  
684 for high-resolution fingerprint recognition. In *2017 IEEE*  
685 *International Conference on Acoustics, Speech and Signal*  
686 *Processing (ICASSP)*, pages 2057–2061. IEEE, 2017. 1
- 687 [29] Yao Tang, Fei Gao, Jufu Feng, and Yuhang Liu. Fingernet:  
688 An unified deep network for fingerprint minutiae extraction.  
689 In *2017 IEEE International Joint Conference on Biometrics*  
690 (*IJCB*), pages 108–116. IEEE, 2017. 1
- 691 [30] Tong Tong, Gen Li, Xiejie Liu, and Qinquan Gao. Image  
692 super-resolution using dense skip connections. In *Proceed-  
693 ings of the IEEE International Conference on Computer Vi-  
694 sion*, pages 4799–4807, 2017. 2, 3
- 695 [31] Zhihao Wang, Jian Chen, and Steven CH Hoi. Deep learning  
696 for image super-resolution: A survey. *IEEE Transactions on*  
697 *Pattern Analysis and Machine Intelligence*, 2020. 2, 3
- 698 [32] W Yin, D Goldfarb, and S Osher. A comparison of three total  
699 variation based texture extraction models. *Journal of Visual*  
700 *Communication and Image Representation*, 18(3):240–252,  
701 2007. 2
- 702 [33] J Zhang, R Lai, and C C J Kuo. Adaptive directional total-  
703 variation model for latent fingerprint segmentation. *IEEE*  
704 *Transactions on Information Forensics and Security*, 8(8):  
705 1261–1273, 2013. 2